FIIG

Functional Imaging and Instrumentation Group

PSD8

8TH INTERNATIONAL CONFERENCE ON POSITION SENSITIVE DETECTORS

8th International Conference on Position Sensitive Detectors

"Advances in Position Sensitive Photodetectors for PET applications"

Alberto Del Guerra

University of Pisa, Department of Physics "E.Fermi"
and INFN, Sezione di Pisa
Largo Bruno Pontecorvo 3, I-56127 PISA (Italy)

e-mail: alberto.delguerra@df.unipi.it
http://www.df.unipi.it/~fiig/

Department of Physics "E.Fermi" University of Pisa

INFN

Istituto Nazionale di Fisica Nucleare - Pisa

Outline

- PET History
- PET Physics and Technology
- PSDs in PET: PMT
- PSDs in PET: Solid State
- Advanced PET Detectors: DOI and TOF
- SiPMs for PET→ The Ultimate Dream??
- Conclusions

First Clinical Positron Imaging Device

1952 - This instrument followed the general concepts of the instrument build in 1950 but included many refinements. It produced both a coincidence scan as well as an unbalance scan. The unbalance of the two detectors was used to create an unbalance image using two symbols to record any unbalance in the single channel rates of the two detectors.

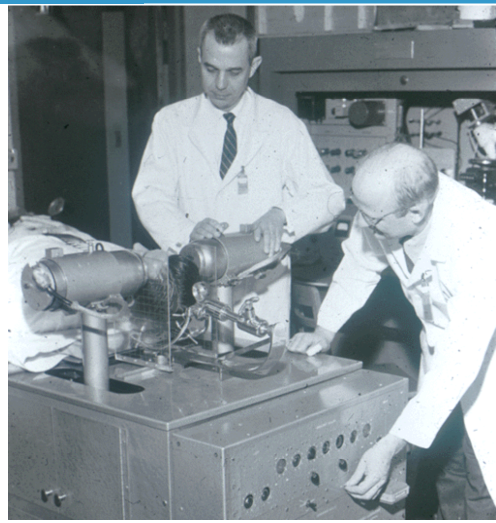

First clinical positron imaging device. **Dr. Brownell** (left) and **Dr. Aronow** are shown with the scanner (1953).

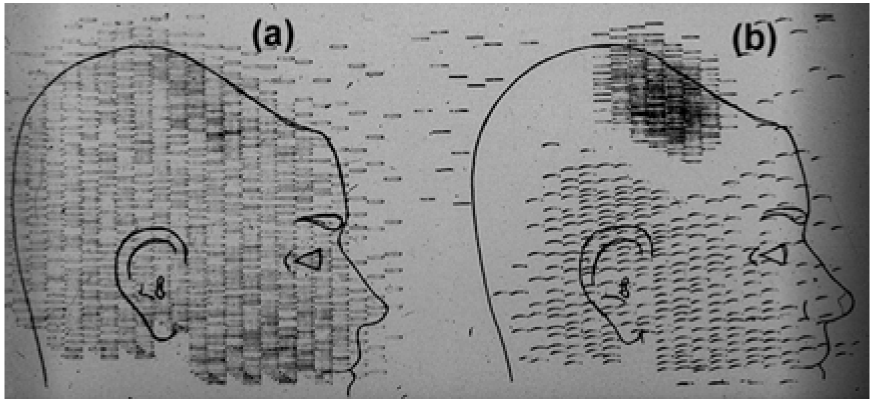

Coincidence and unbalance scans of patient with recurring brain tumor. Coincidence scan (a) of a patient showing recurrence of tumor under previous operation site, and unbalance scan (b) showing asymmetry to the left. (Reproduced from Brownell and Sweet 1953).

1957 - The Anger Camera

Principle:

many photomultiplier tubes "see" the same large scintillation crystal; an electronic circuit decodes the coordinates of each event

Hal Anger (Berkeley)
Developer of the scintillation camera

PET intrinsic limitations

- PET History
- PET Physics and technology
- PSDs in PET: PMT
- PSDs in PET: solid state
- Advanced PET detectors: DOI and TOF
- SiPMs for PET
- Conclusions

Positron range

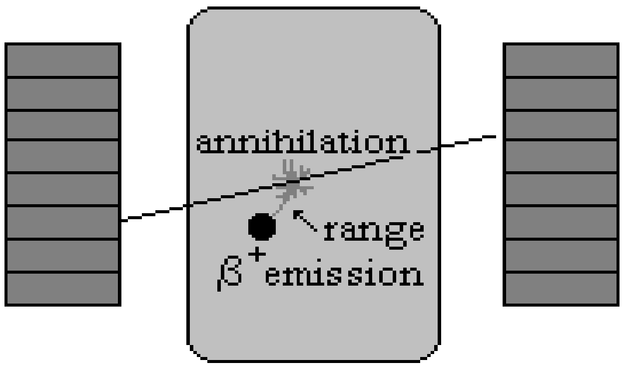

(a)

» **Depends on the radioisotope**

	<E_c > (MeV)	*<Range> in water*	*FWHM (mm)*
^{18}F	**0.242**	**1.4 mm**	**0.22**
^{11}C	**0.385**	**1.7 mm**	**0.28**
^{68}Ga	**0.740**	**3.0 mm**	**1.35**

Angular deviation

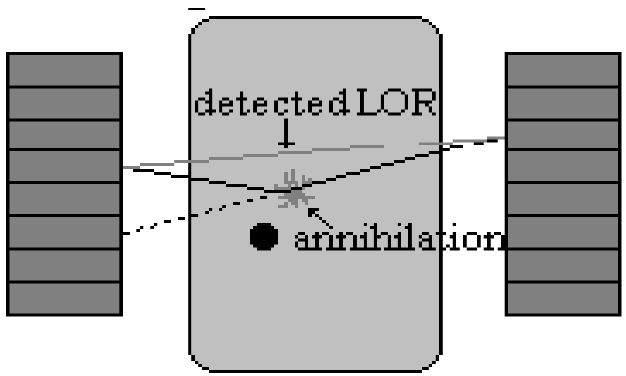

(b)

» **Depends on the ring radius**
(1.8 mm for a 400 mm radius)

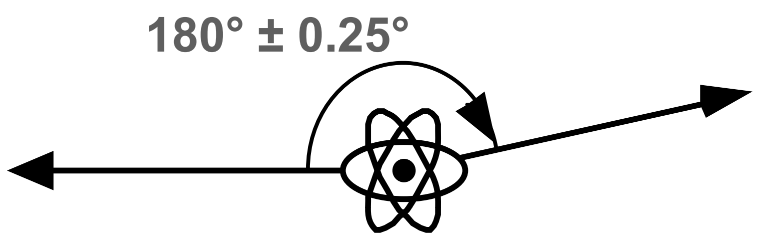

PET spatial resolution / 1

$$\text{FWHM} = 1.2\sqrt{(d/2)^2 + b^2 + (0.0022D)^2 + r^2 + p^2}$$

(mm) — Crystal size; Coding; Non collinearity; Positron range; Parallax error

1.2	:	Degradation due to reconstruction algorithm
d	:	Crystal pitch
b	:	Coding error
D	:	Detector separation
r	:	effective source size (including positron range)
p	:	Parallax error

* Derenzo & Moses, "Critical instrumentation issues for resolution <2mm, high sensitivity brain PET", in *Quantification of Brain Function, Tracer Kinetics & Image Analysis in Brain PET*, ed. Uemura et al, Elsevier, 1993, pp. 25-40.

From man to mice

- PET History
- PET Physics and technology
- PSDs in PET: PMT
- PSDs in PET: solid state
- Advanced PET detectors: DOI and TOF
- SiPMs for PET
- Conclusions

Human PET

microPET

human

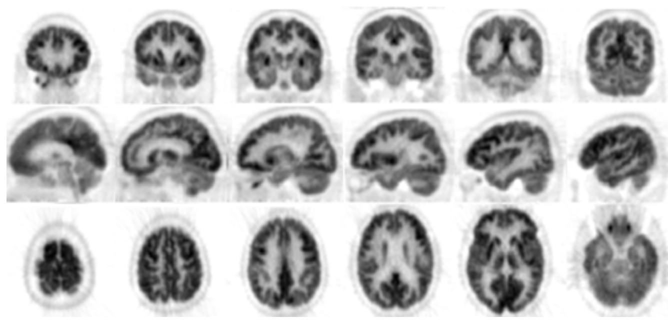

*Images courtesy of Simon Cherry, UCLA

mouse

rat

mouse

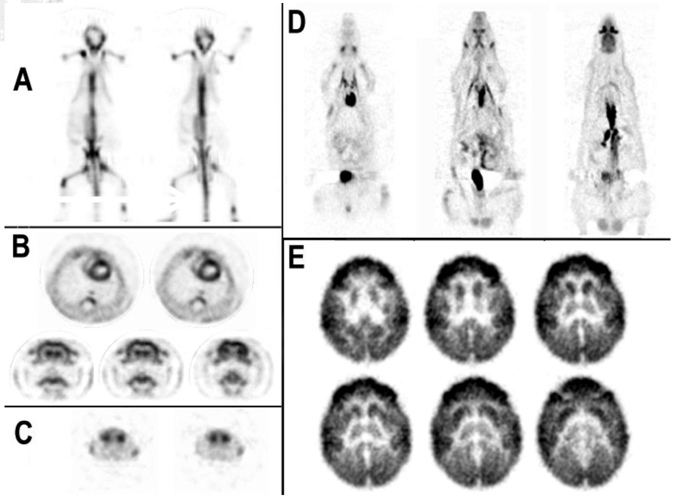

rat

infant monkey

Spatial resolution requirements

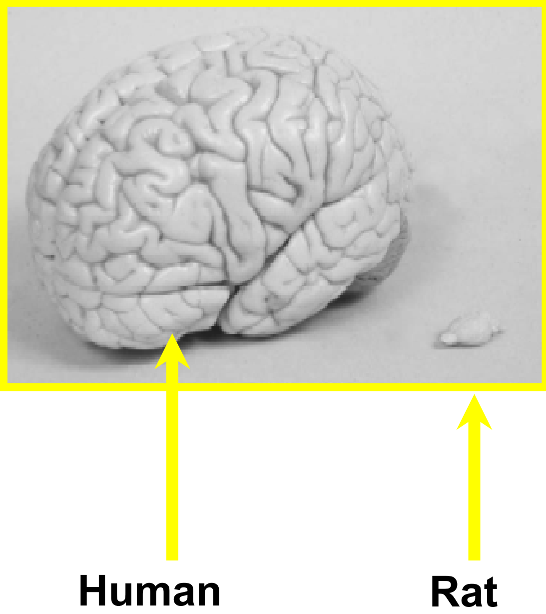

	Man	Rat	Mouse
Body weight	**~70 kg**	**~200 g**	**~20 g**
Brain (cortex apex-temporal lobe)	**~105 mm**	**~10 mm**	**~6 mm**
Heart	**~300 g**	**~1 g**	**~0.1 g**
Aorthic cannula (∅)	**~ 30 mm**	**1.5 – 2.2 mm**	**0.9 - 1.3 mm**

Required spatial resolution:

- Small size detectors (high pixellization)
- Individual detectors or “perfect” coding

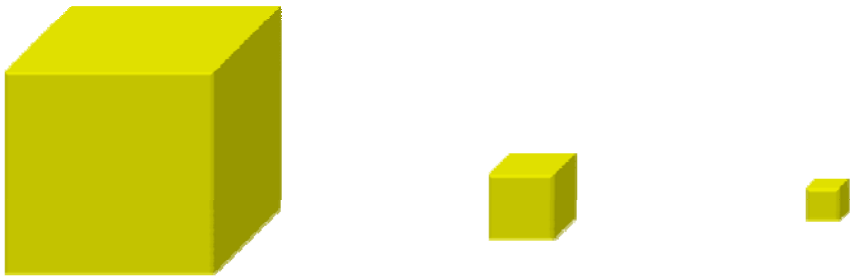

6 mm FWHM (200 mm^3)

2 mm FWHM (8 mm^3)

$\leq$ 1 mm FWHM ($\leq$ 1 mm^3)

PET spatial resolution / 2

- PET History
- PET Physics and technology
- PSDs in PET: PMT
- PSDs in PET: solid state
- Advanced PET detectors: DOI and TOF
- SiPMs for PET
- Conclusions

The spatial resolution of a PET scanner is limited by technology…

➔ *Crystal size, coding* etc.

Contribution of the photodetector

…and from Physics➔Non-collinearity, positron range

With a "perfect" technology a clinical PET scanner (40 cm radius) cannot have a spatial resolution better than 1.8 – 2.0 mm FWHM (present best 4 – 6 mm FWHM), but is limited by quantum noise!

For small animal scanners the theoretical limit is around 0.7 – 0.8 mm FWHM (at present 1.2 – 2.0 mm).

The coding problem is more critical for small detector separation systems such as small animal instrumentation

→ Advanced photodetectors!

1986 - The block detector

- PET History
- PET Physics and technology
- PSDs in PET: PMT
- PSDs in PET: solid state
- Advanced PET detectors: DOI and TOF
- SiPMs for PET
- Conclusions

In a block detector, a 2D array of crystals are attached to 4 PMTs. Usually the array will be cut from a single crystal and the cuts filled with light-reflecting material. When a photon is incident on one of the crystals, the resultant light is shared by all 4 PMTs. Information on the position of the detecting crystal may be obtained from the PMT outputs by calculating the following ratios and comparing them to pre-set values:

$$R_x = \frac{A+B}{A+B+C+D}$$

$$R_y = \frac{A+C}{A+B+C+D}$$

where A, B, C and D are the fractional amounts of light detected by each PMT

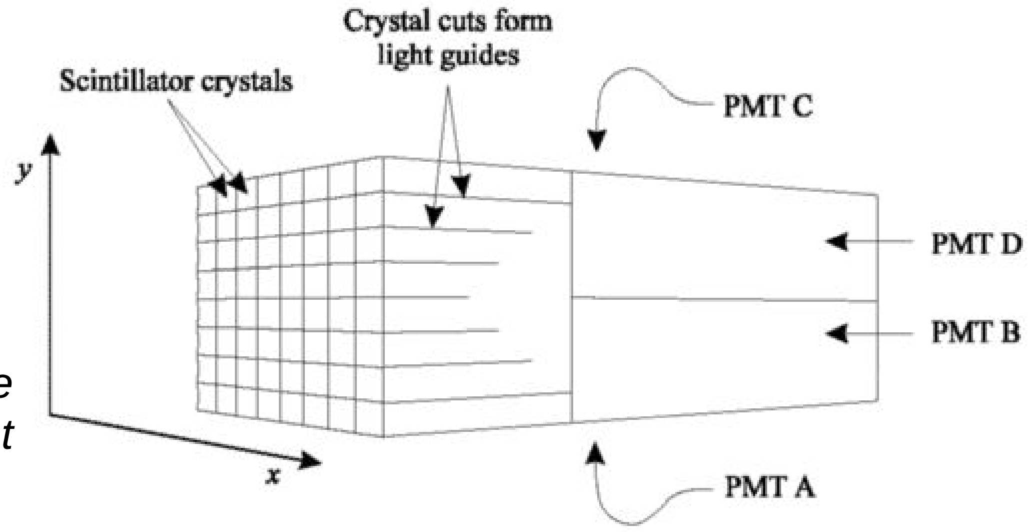

In 1986 the introduction of the block detector by Mike Casey and Ronald Nutt, changed the world of nuclear imaging. *Almost all dedicated tomographs built since1986 have used some forms of the block detector.*

Block detector original paper

- PET History
- PET Physics and technology
- PSDs in PET: PMT
- PSDs in PET: solid state
- Advanced PET detectors: DOI and TOF
- SiPMs for PET
- Conclusions

IEEE Transactions on Nuclear Science, Vol. 33, No. 1, February 1986

A MULTICRYSTAL TWO DIMENSIONAL BGO DETECTOR SYSTEM FOR POSITRON EMISSION TOMOGRAPHY

M. E. Casey and R. Nutt

Computer Technology and Imaging
215 Center Park Drive
Knoxville, Tennessee

ABSTRACT

This paper presents a discussion of a new multicrystal detector system as it is implemented in Positron Emission Tomography. The system consists of a 32 x 8 matrix of BGO crystals, a tuned light pipe, and four photomultipliers. The electronics that decodes the position consists of fast preamps, gated integrators, and level comparators. This detector represents a major development toward reducing the cost of PET.

INTRODUCTION

In recent years, several investigators [1,2,3] have reported on the advantages of using small, tightly packed crystals in the design of Positron Tomographs. Small closely packed crystals increase both the sampling frequency and the detection efficiency. Designs that achieve these advantages have been relatively expensive due to the multiplicity of photomultipliers and electronics need to process the signal from the crystals. To overcome the cost disadvantage, research in recent years has

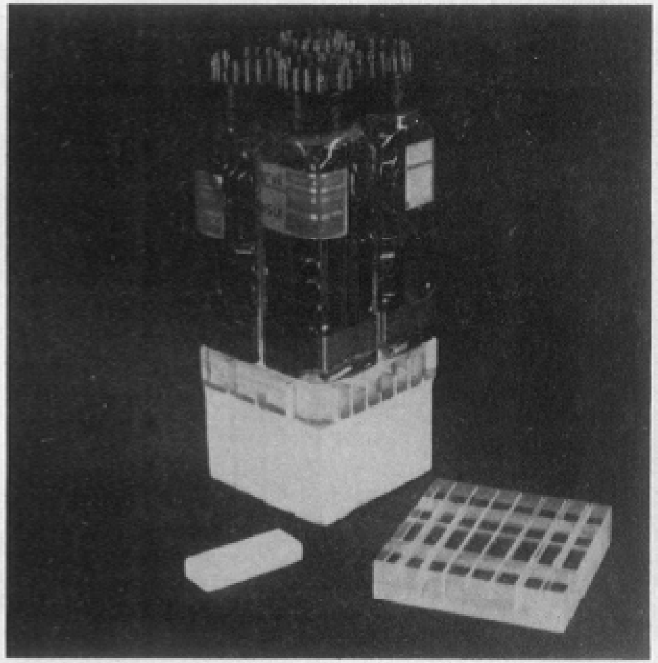

Figure 1. The "BLOCK" detector.

PSPMT's + matrix of scintillators first application of R2486

- PET History
- PET Physics and technology
- PSDs in PET: PMT
- PSDs in PET: solid state
- Advanced PET detectors: DOI and TOF
- SiPMs for PET
- Conclusions

IEEE Transactions on Nuclear Science, Vol. 33, No. 1, February 1986

DESIGN OF A MOSAIC BGO DETECTOR SYSTEM FOR POSITRON CT

H.Uchida, T.Yamashita, M.Iida, S.Muramatsu

Hamamatsu Photonics K.K.
1126-1 Ichino-cho Hamamatsu-City, Japan

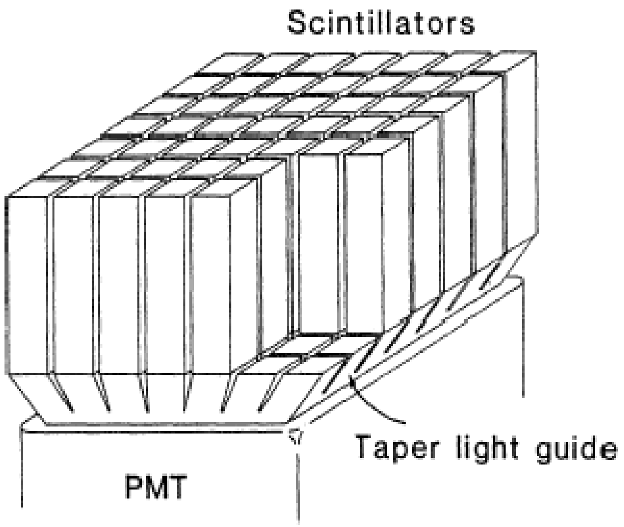

Fig.9 Schematic of detector head using taper light guide.

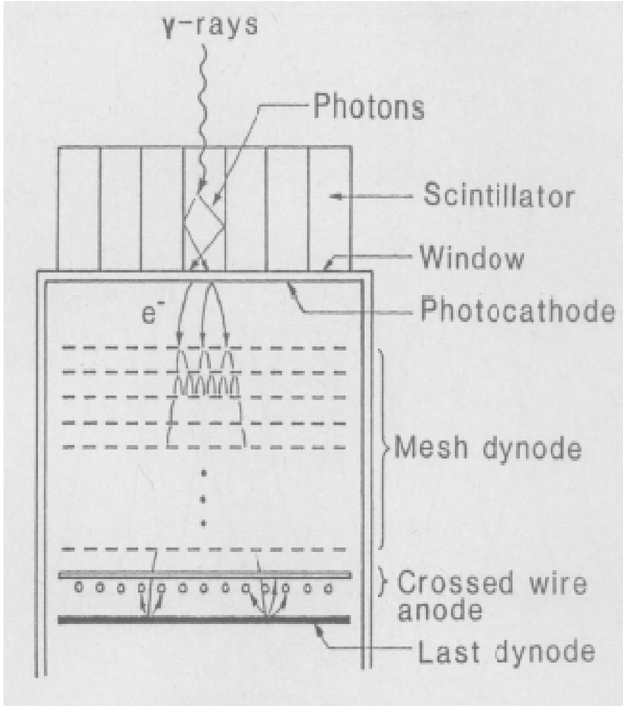

Fig.1 Schematic of the mosaic BGO detector

→ R2487 …

From the block detector to PSPMT's

"*Block detector*"

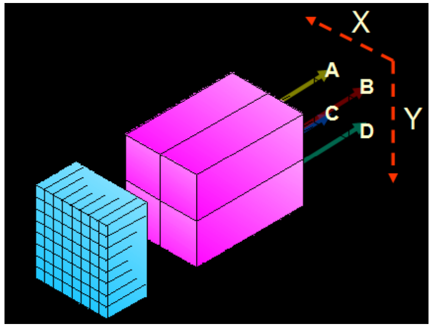

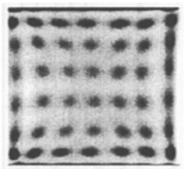

- Large "b"
- Limitations on minimum "d"

"*1st generation*" PSPMT

Hamamatsu
PS-PMT R2486.
- 50 mm Ø active area
- 16 x + 16 y anodes

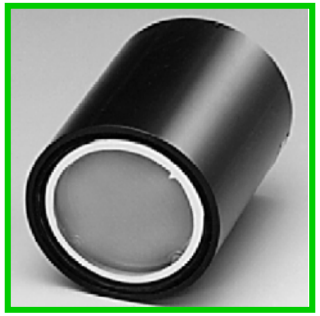

Small crystals can be used (down to d = 1mm)

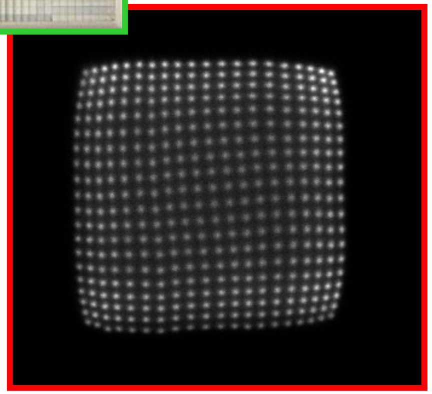

Used in the YAP-(S)PET (Univ of Ferrara Italy,1996)

Flood field irradiation (511 keV) of a matrix of scintillator YAP:Ce, read by a Hamamatsu R2486 (resistive readout)

PSPMT's + matrix of scintillators

- PET History
- PET Physics and technology
- PSDs in PET: PMT
- PSDs in PET: solid state
- Advanced PET detectors: DOI and TOF
- SiPMs for PET
- Conclusions

1958 IEEE TRANSACTIONS ON NUCLEAR SCIENCE, VOL. 43, NO. 3, JUNE 1996

Use of a YAP:Ce Matrix Coupled to a Position-Sensitive Photomultiplier for High Resolution Positron Emission Tomography

A. Del Guerra[1,2], F. de Notaristefani[3], G. Di Domenico[2,4], M. Giganti[5], R. Pani[6], A. Piffanelli[5], A. Turra[1], G. Zavattini[1,2]

[1] Dipartimento di Fisica, Università di Ferrara, via Paradiso 12, I-44100 Ferrara, Italy
[2] INFN, Sezione di Ferrara, via Scienze, I-44100 Ferrara, Italy
[3] INFN, Sezione di Roma I and Dipartimento di Fisica, Università di Roma III, Italy
[4] Dottorato di Medicina Nucleare, Cattedra di Medicina Nucleare, Facoltà di Medicina e Chirurgia, Corso Giovecca 203, I-44100 Ferrara, Italy
[5] Cattedra di Medicina Nucleare, Facoltà di Medicina e Chirurgia, Corso Giovecca 203, I-44100 Ferrara, Italy
[6] Dipartimento di Medicina Sperimentale, Università "La Sapienza" Roma, Italy

R2486 based small animal scanner YAP-(S)PET II

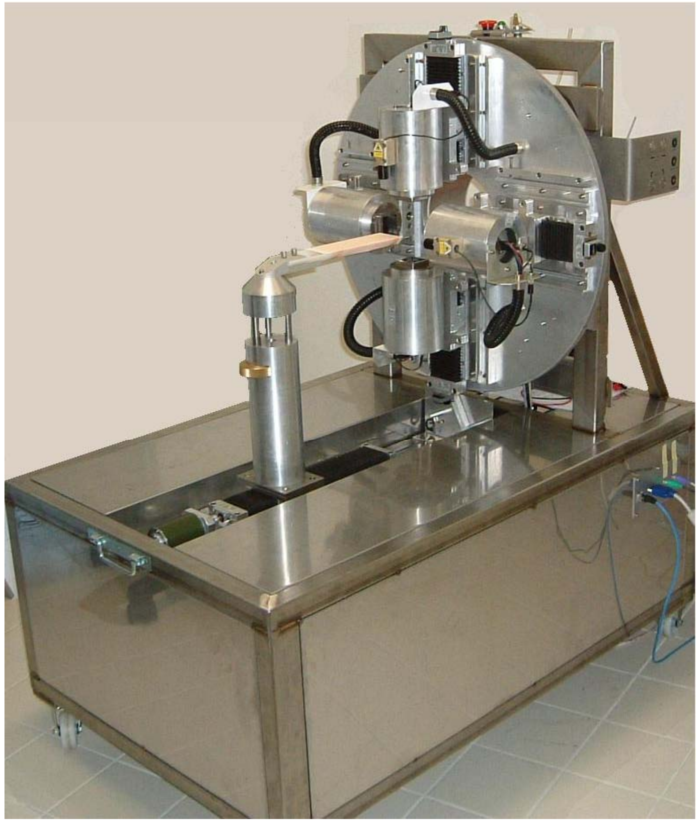

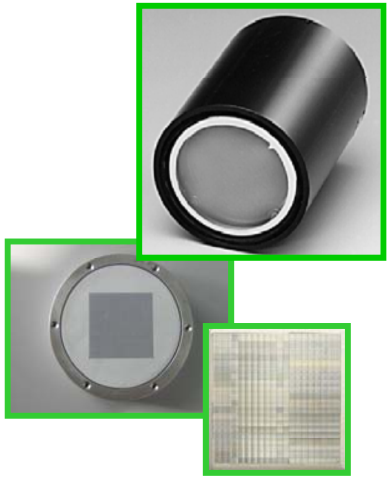

Hamamatsu R2486 (3” Ø)

YAP:Ce matrix (4 × 4 cm^2)
400 finger crystals
2.0 mm × 2.0 mm × 25 mm

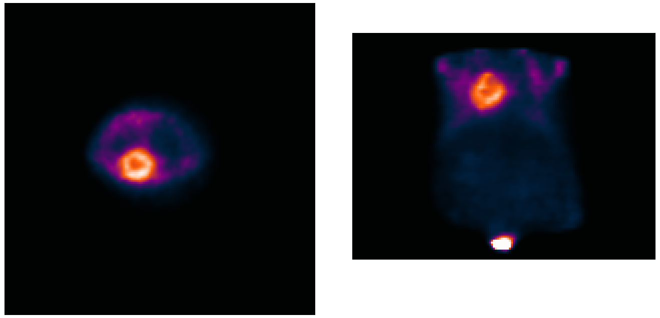

Mouse heart metabolism with ^{18}F-FDG (2008)

Due to the YAP:Ce crystal and the planar geometry the scanner can perform SPECT too, by adding a parallel hole collimator in front of each matrix

First publication: *A.Del Guerra, G.Di Domenico, M.Scandola, G.Zavattini, "High spatial resolution small animal YAP-PET", Nucl. Instr. Methods A, 1998, A409, 537-541.*

“2^{nd} *generation*” PSPMT

The PS-PMT R8520-C12 by Hamamatsu.

- Overall size: 25.7 mm × 25.7 mm
- Active area: 22 mm × 22 mm
- 6 x + 6 y anodes

Advantages

- Higher packing fraction with respect to round tubes (up to 73%)
- **Good spatial resolution**
- Good uniformity
- Easy to use with a resistive chain (4 channels)

Drawbacks

- **Small active area** for each tube
- Dead area between adjacent PMTs

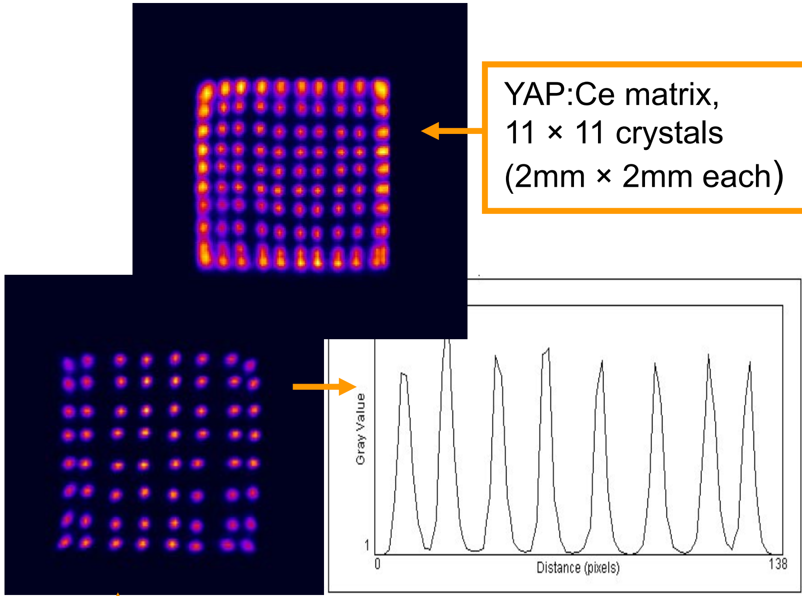

YAP:Ce matrix, 11 × 11 crystals (2mm × 2mm each)

CsI:Tl matrix, 8 × 8 crystals (2.8 mm × 2.8 mm each)

Flood field irradiation (122 keV) of two matrices of scintillators (CsI:Tl, left and YAP:Ce, top) read by a Hamamatsu R8520-C12 (single tube, resistive readout)

Used for small animal imaging!

1992-1993 - the advent of LSO:Ce

- PET History
- PET Physics and technology
- PSDs in PET: PMT
- PSDs in PET: solid state
- Advanced PET detectors: DOI and TOF
- SiPMs for PET
- Conclusions

In this last twenty years most of the additional improvement in PET technique was due to the introduction of new scintillating materials such as LSO

IEEE TRANSACTIONS ON NUCLEAR SCIENCE, VOL. 39, NO. 4, 1992

Cerium-doped Lutetium Oxyorthosilicate: A Fast, Efficient New Scintillator

C. L. Melcher and J. S. Schweitzer
Schlumberger-Doll Research, Old Quarry Rd., Ridgefield, CT 06877-4108

IEEE TRANSACTIONS ON NUCLEAR SCIENCE, VOL. 40, NO. 4, AUGUST 1993 1045

Evaluation of Cerium Doped Lutetium Oxyorthosilicate (LSO) Scintillation Crystal for PET

F. Daghighian, P. Shenderov, K.S. Pentlow, M.C. Graham, B. Eshaghian
Department of Medical Physics, Memorial Sloan-Kettering Cancer Center, 12 75 York Ave, New York N.Y.10021

C.L. Melcher, J.S. Schweitzer
Schlumberger-Doll Research, Old Quarry Rd., Ridgefield, CT, USA 06877

LSO:Ce – hystorical results

- PET History
- PET Physics and technology
- PSDs in PET: PMT
- PSDs in PET: solid state
- Advanced PET detectors: DOI and TOF
- SiPMs for PET
- Conclusions

Table 1 Properties of LSO, BGO and NaI(Tl)

	LSO	BGO	NaI(Tl)
Relat. light intensity	75	15	100
Peak wavelenght	420 nm	480 nm	410 nm
Decay constant (ns)	12 (30%); 42 (70%)	300	230
Density (g/cc)	7.4	7.13	3.67
Effective atomic No.	66	75	51
Index of refraction	1.82	2.15	1.85
Hygroscopic?	no	no	yes
Rugged?	yes	yes	no

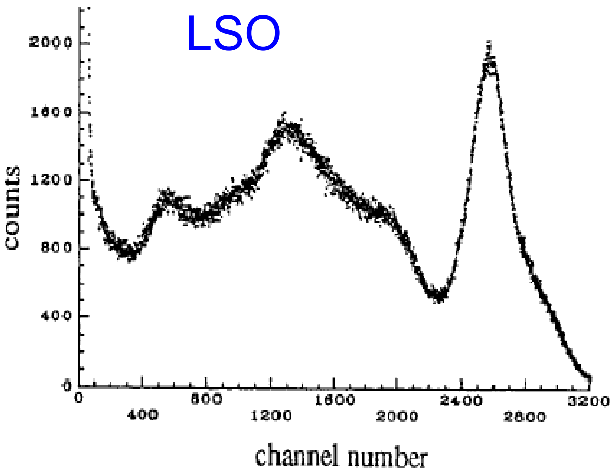

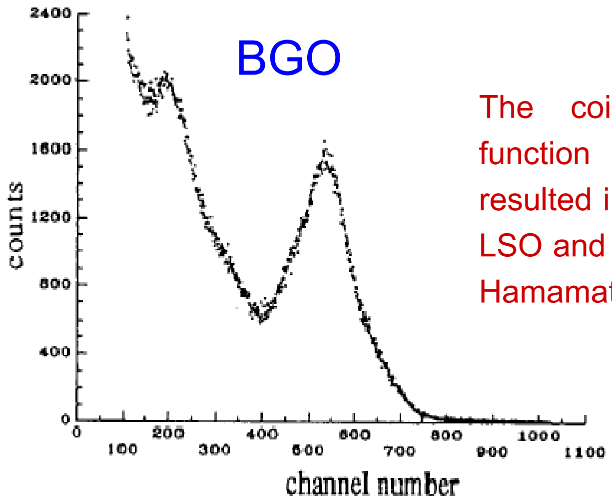

The spectrum of Ge-68 in a small piece of LSO crystal (2x2x10 m). This crystal is coupled to a PMT via its 2x2 mm side.

Timing

The coincidence time spread function for LSO and BGO resulted in a FWHM of 0.95 ns for LSO and 2.2 ns for BGO using wo Hamamatsu R647-04 PMTs

PSPMT's + fibers + LSO: MicroPET

IEEE TRANSACTIONS ON NUCLEAR SCIENCE, VOL. 44, NO. 3, JUNE 1997 1161

MicroPET: A High Resolution PET Scanner for Imaging Small Animals

S.R. Cherry[1], *Member, IEEE*, Y. Shao[1], R.W. Silverman[1], *Senior Member, IEEE*, K. Meadors[1], S. Siegel[1], *Member, IEEE*, A. Chatziioannou[1], *Member, IEEE*, J.W. Young[2], W.F. Jones[2], J.C. Moyers[2], *Member, IEEE*, D. Newport[2], A. Boutefnouchet[1], T.H. Farquhar[1], *Member, IEEE*, M. Andreaco[2], M.J. Paulus[2], *Member, IEEE*, D.M. Binkley[2], *Member, IEEE*, R. Nutt[2], *Fellow, IEEE* and M.E. Phelps[1]

[1]Crump Institute for Biological Imaging, Dept. of Molecular and Medical Pharmacology, UCLA, Los Angeles, CA
[2]CTI PET Systems Inc., Knoxville, TN.

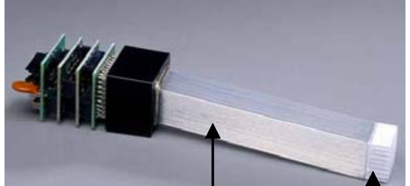

8 × 8 square fibres bundle (2 mm)

8×8 LSO matrix

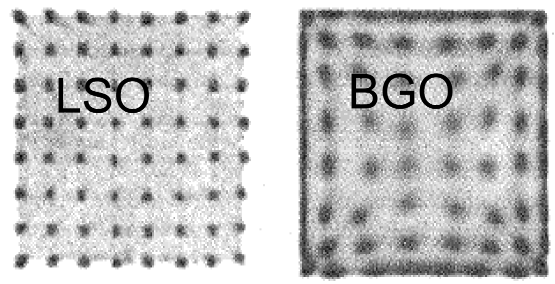

Figure 2: Position histograms from LSO microPET detector (left) and a conventional BGO block detector (right).

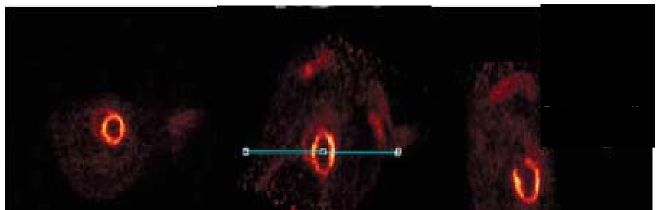

Rat heart 18F-FDG

One-to-one coupling with APD's

- PET History
- PET Physics and technology
- PSDs in PET: PMT
- PSDs in PET: solid state
- Advanced PET detectors: DOI and TOF
- SiPMs for PET
- Conclusions

IEEE Transactions on Nuclear Science, Vol. 33, No. 1, February 1986

A BISMUTH GERMANATE-AVALANCHE PHOTODIODE MODULE DESIGNED FOR USE IN HIGH RESOLUTION POSITRON EMISSION TOMOGRAPHY

A.W. Lightstone & R.J. McIntyre
RCA Inc., Box 1200, New Products Divsion
Ste-Anne-de-Bellevue, Québec, Canada H9X 3L3
and
R.Lecomte & D.Schmitt
Dept. of Nuclear Medicine & Radiobiology,
University of Sherbrooke, Sherbrooke, Québec
Canada J1H 5N4

Abstract

A light-tight, hermetically sealed module for use in high resolution positron emission tomography systems is described. The module has external dimensions 3.8x13.2x33 mm and contains two 3x5x20 Bismuth Germanate (BGO) scintillators, each with its own 3x3 mm silicon avalanche photodiode. When stacked, the vertical packing fraction is 80%. As measured with a ^{137}Cs (662 keV) source, the typical energy resolution is 20% at 22°C, reducing to 16% at 0°C. The single detector time resolution for the ^{22}Na gamma at 511 keV is typically less 20 ns at 22°C, reducing to less than 15 ns at 0°C. Further cooling does not improve the performance since the emission time of light from BGO increases at lower temperature. Preliminary results with Gadolinium Orthosilicate show similar energy resolution, better timing resolution (under 10 ns), but as is known, a slightly poorer photofraction and stopping power.

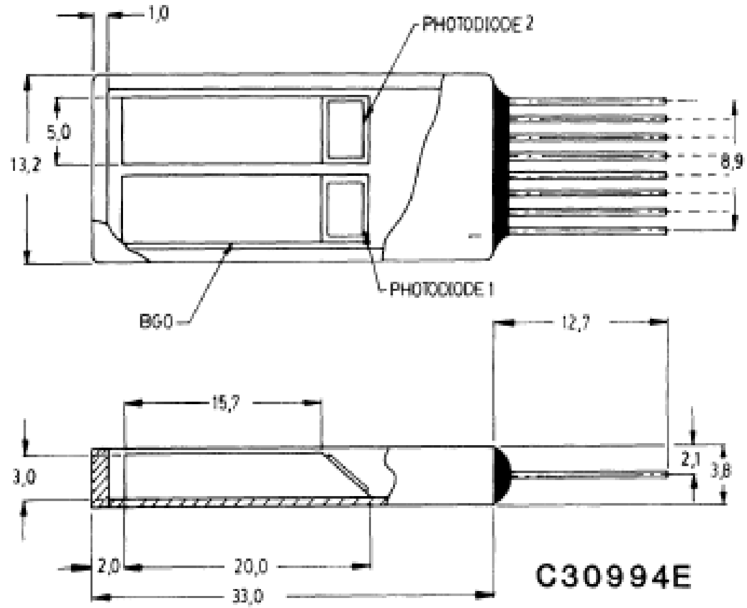

C30994E

Example of application

- PET History
- PET Physics and technology
- PSDs in PET: PMT
- PSDs in PET: solid state
- Advanced PET detectors: DOI and TOF
- SiPMs for PET
- Conclusions

1952 IEEE TRANSACTIONS ON NUCLEAR SCIENCE, VOL. 43, NO. 3, JUNE 1996

Initial Results from the Sherbrooke Avalanche Photodiode Positron Tomograph

R. Lecomte, J. Cadorette, S. Rodrigue, D. Lapointe,
D. Rouleau, M. Bentourkia, R. Yao and P. Msaki
Department of Nuclear Medicine and Radiobiology,
University of Sherbrooke, Sherbrooke (Québec), Canada J1H 5N4

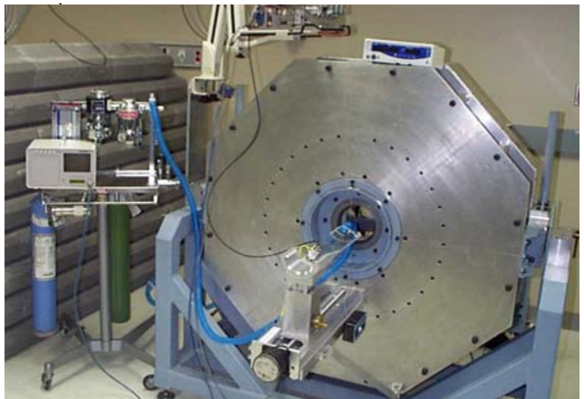

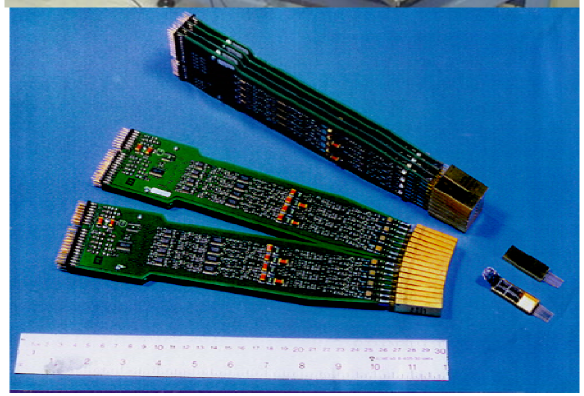

Scintillators	**BGO**
Photodetectors	**Avalanche Photodiode**
Crystal size	**$3 \times 5 \times 20$ mm^3**
Nb of detectors	**512 / 32 cassettes (2×8 array)**
Detector rings	**2 (1 ring of modules)**
Ring Diameter	**310 mm**
Animal Port	**135 mm**
Field-of-view	**118 mm∅ × 10.5 mm**
Nb of slices	**3 (2 directs, 1 cross)**
Coinc Time Window	**20-40 ns (~25 ns)**

Whole-body PET Scan
$^{18}F^{-}$ + ^{18}FDG, 250 g rat
(Sherbrooke APD PET Scanner)

Implementation with a matrix of APD from Hamamatsu

APD

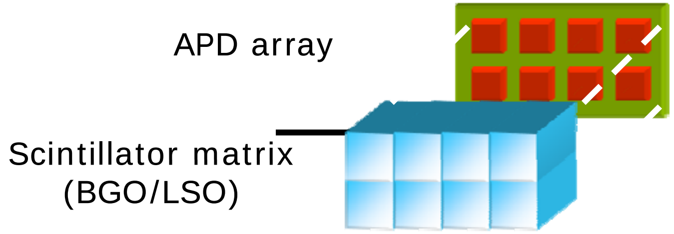

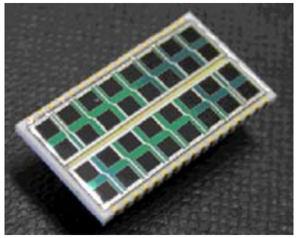

Implemented on MADPET II

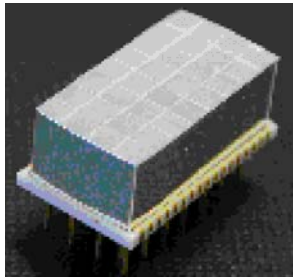

+ High spatial resolution
+ No Pile-up
+ No scattering in the crystals
- Expensive
- Many channels
- Difficult tuning

The detector module is composed by a matrix of 8×4 LSO crystals readout by a Hamamatsu S8550 (*Pichler B., IEEE TNS 45 (1998) 1298-1302)*

Today: advanced light sharing photodetectors

- PET History
- PET Physics and technology
- PSDs in PET: PMT
- PSDs in PET: solid state
- Advanced PET detectors: DOI and TOF
- SiPMs for PET
- Conclusions

"light sharing" technique:
Hybrid position sensitive APD

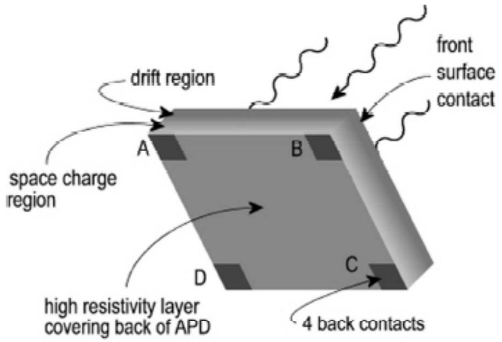

$$X=\frac{(B+C)-(A+D)}{(A+B+C+D)} \quad Y=\frac{(A+B)-(C+D)}{(A+B+C+D)}$$

Picture of a HPS-APD with four output connectors

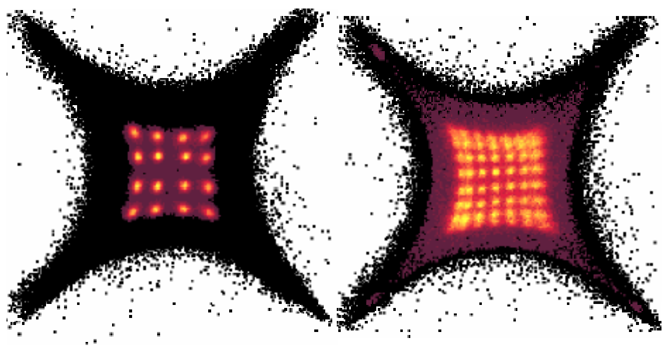

Flood field image (^{241}Am, 60 keV) obtained with a 4x4 and 8x8 CsI(Tl) scintillating matrices

"light sharing" technique:
Multi Anode flat panel PMT

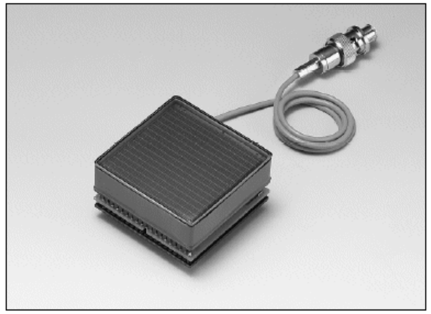

MA-PMT (8×8 ch's)
Hamamatsu H8500
Active area 49 mm x 49 mm

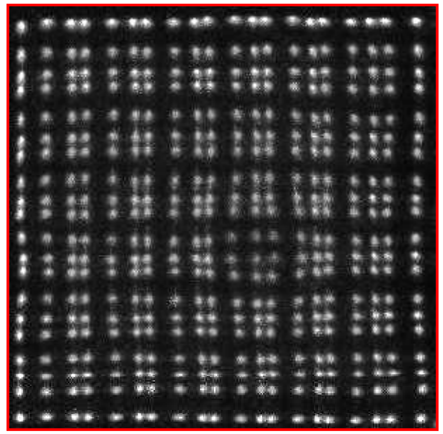

Flood field image (511 keV) obtained with a 20x20 YAP:Ce scintillating matrix (resistive readout)

Not only photodetectors / 1: Quad HIDAC scanner

- PET History
- PET Physics and technology
- PSDs in PET: PMT
- PSDs in PET: solid state
- Advanced PET detectors: DOI and TOF
- SiPMs for PET
- Conclusions

Technology

HIDAC: **HI**gh **D**ensity **A**valanche gas **C**hamber

(multi-wire proportional gas chamber with the addition of a conversion/multiplication structure)

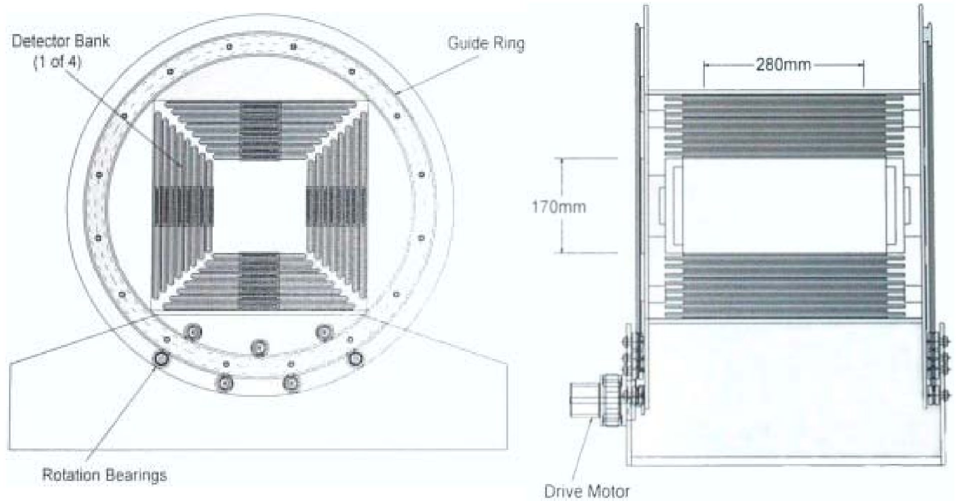

Images

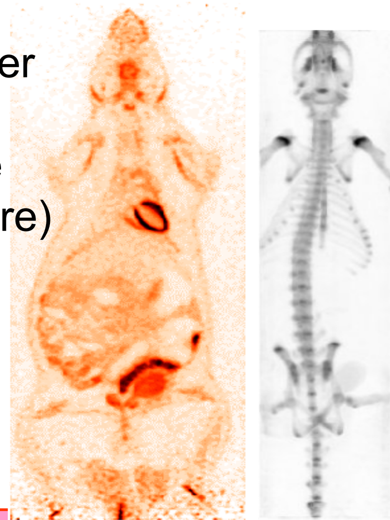

Left: Rat 18F-FDG scanning

Right: bone scanning after the injection of 17MBq of ^{18}F (OSEM reconstruction)

IEEE TRANSACTIONS ON NUCLEAR SCIENCE, VOL. 46, NO. 3, JUNE 1999
A 3D HIDAC-PET Camera with Sub-millimetre Resolution for Imaging Small Animals
A.P. Jeavons, R.A. Chandler, C.A.R. Dettmar

SiliPET (proof of principle)

Mesurements with a ≈ 1 mm diameter ^{22}Na source. The MEGA detector was devided into two stacks 2 cm apart made by of 5 and 6 prototype layers. Coincidence events between top and bottom stacks were taken and logical XOR for layers in each stack was implemented. Due to the 1 micosecond time window (MEGA electronics) a low activity source was used to keep random coincidences low.

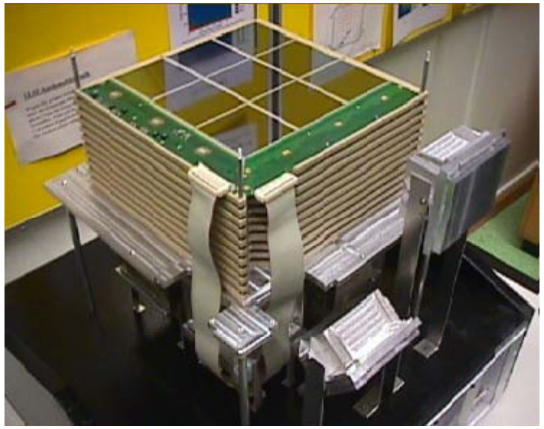

MEGA prototype tracker: 11 doublesided Si 19 X 19 cm^2 detector layers. Si wafer parameters: thickness = 0.5mm; strip pitch = 470 microns.

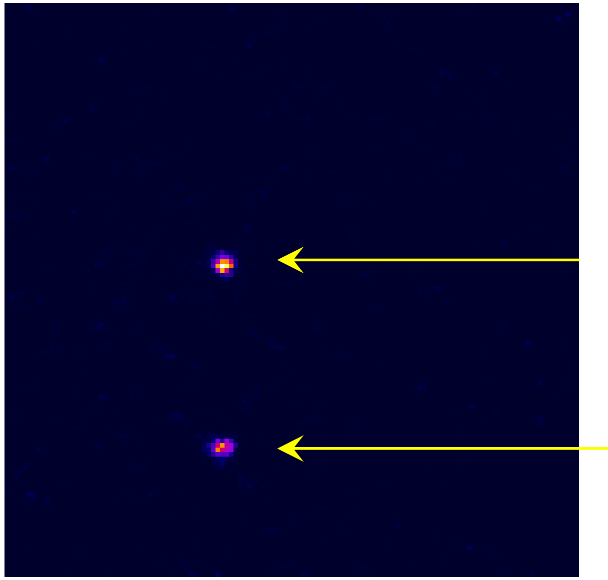

Reconstructed with a focal plane ray tracing method

0.0 cm

1.0 cm

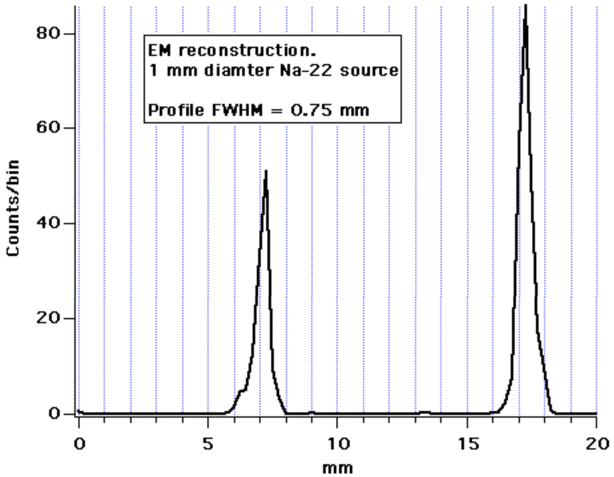

Profile through the sources of the composite image. FWHM = 0.75 mm. Source diameter = 1 mm. Same results are obtained by simulating a uniform 1 mm diameter sphere.

SiliPET (design)

The **SiliPET** small animal PET scanner is composed by 4 detector stacks each composed of 40 planar, 1 mm thick, **double sided silicon strip detectors** with 128 strips on each side to permit the measurement of the two coordinates on the plane of the detector.

The third coordinate, the depth of interaction, is given by the identification of the detector plane in which the interaction takes place with a precision determined by its thickness.

All planes in a stack are in ***exclusive OR*** imposing therefore a single interaction.

- ***Stack layer*** → **DOI mesurement**
- ***Compton interaction*** → **accurate position**
- ***No parallax*** → **compact and high sensitivity**
- ***No energy mesurement*** → **no ADCs**

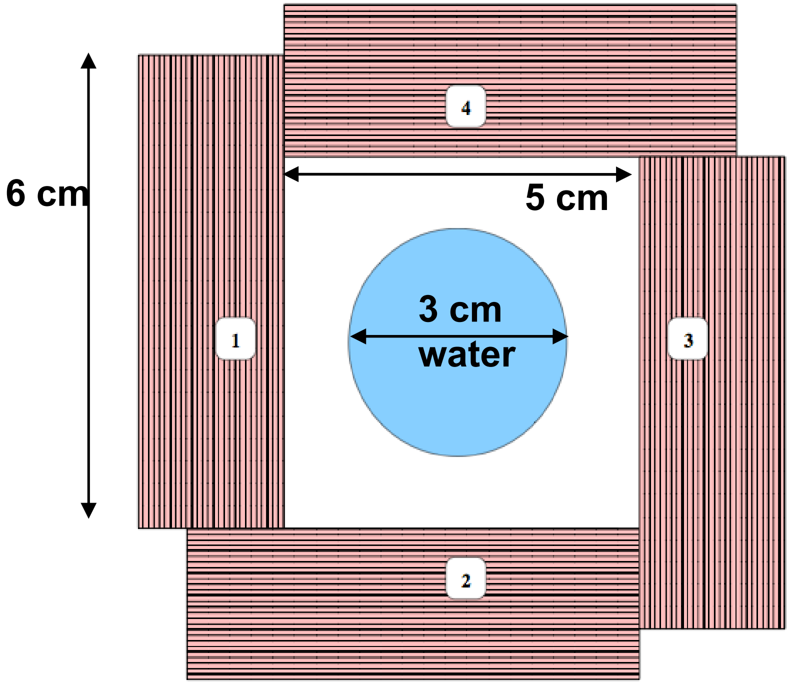

Di Domenico G, Zavattini G, Cesca N, Auricchio N, Andritschke R, Schopper F and Kanbach G, 2007, SiliPET: an ultra-high resolution design of a small animal PET scanner based on stacks of double-sided silicon strip detector *Nucl. Instrum. Methods Phys. Res.* A **571** 22–5

Parallax error: continuous DOI measurement

Differential measurement DUAL APD

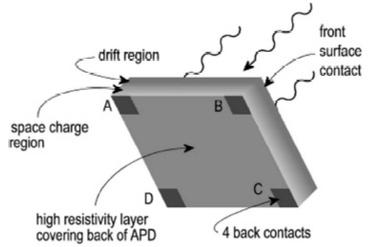

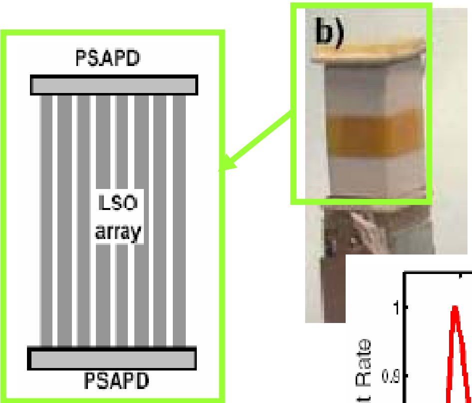

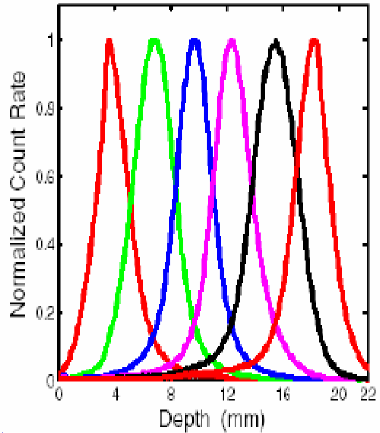

Resolution DOI measurement: 3 mm FWHM

Burr et al, *IEEE NSS/MIC* 2003

Differential measurement SiPD-PMT

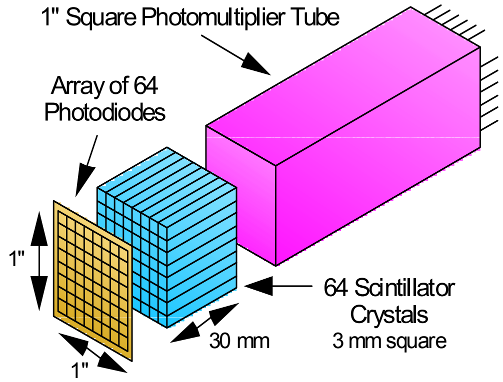

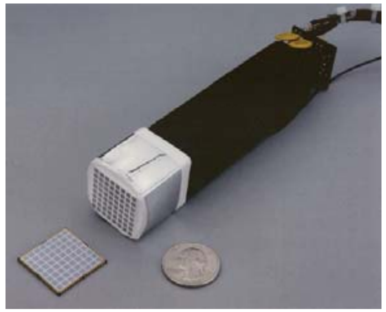

- The PMT (single anode) provides the timing
- The SiPD (8x8) detects the crystal
- The ratio SiPD/(SiPD+PMT) returns the DOI

An LSO scintillator array for a PET detector module with depth of interaction measurement
JS Huber et al IEEE TNS, Vol. 48(3) (2001), pp. 684-688.

Parallax error: pseudo-discrete DOI measurement

"Pulse Shape" discrimination "Phoswich detector"

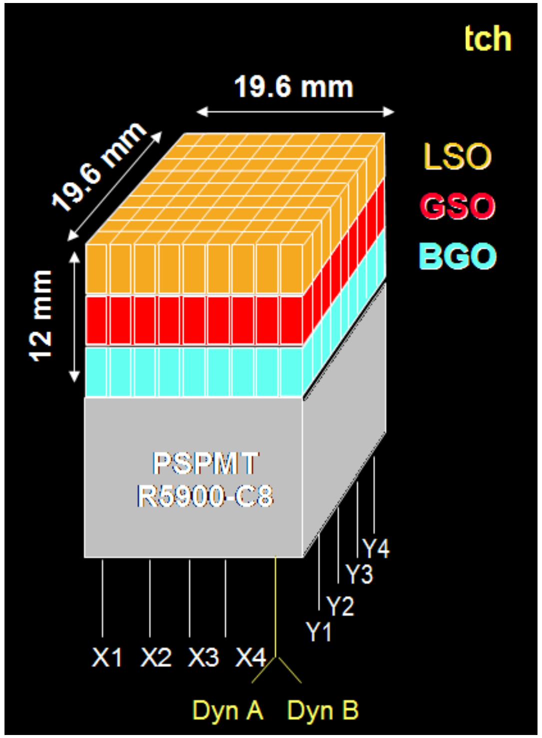

Used in the GE Xplore

Used in the ClearPET (LYSO/LuYAP)

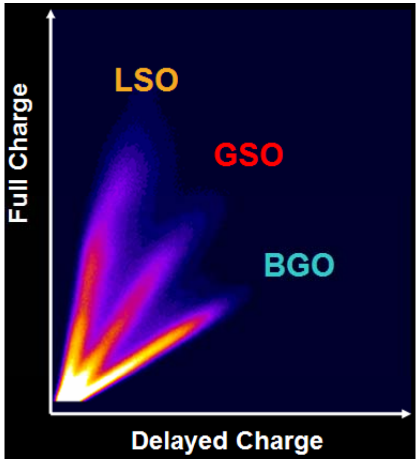

Seidel et al, *IEEE TNS* 46 (1998) 485

"Light coding"

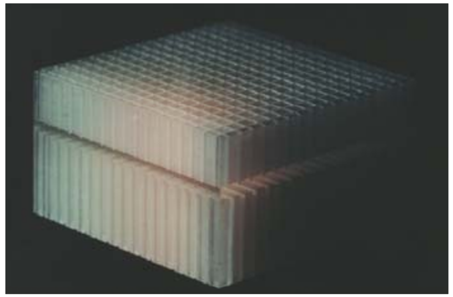

Implemented on ANIPET (Montreal)

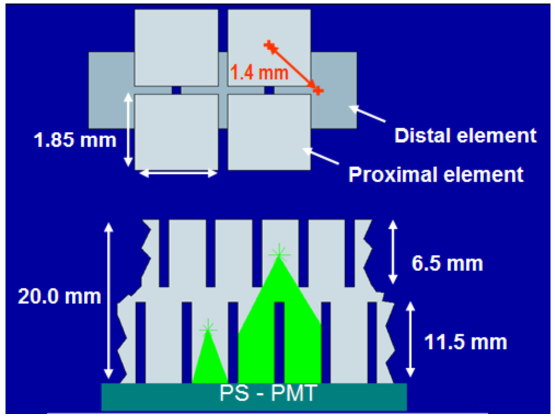

TOF PET

- PET History
- PET Physics and technology
- PSDs in PET: PMT
- PSDs in PET: solid state
- **Advanced PET detectors: DOI and TOF**
- SiPMs for PET
- Conclusions

R. Allemand, C. Gresset, and J. Vacher, "Potential advantages of a Cesium Flouride scintillator for time-of-flight positron camera," *J. Nucl. Med.*, vol. 21, pp. 153-155, 1980.

...on Emission Tomograph Utilizing Photon Time-of-Flight Information

MICHEL M. TER-POGOSSIAN, DAVID C. FICKE, MIKIO YAMAMOTO, AND JOHN T. HOOD, SR.

Abstract—The physical characteristics and some imaging capabilities of Super PETT I, a positron emission tomograph utilizing time-of-flight (TOF) in its image reconstruction process were assessed experimentally by means of measurements carried out in phantoms and clinical imaging studies. The performance characteristics assessed included sensitivity, spatial resolution, image improvements resulting from time-of-flight information utilization, system dead time, and linearity. The clinical examples included imaging of the brain, the heart, the liver, and a demonstration of Super PETT I's capability of achieving cardiac gating.

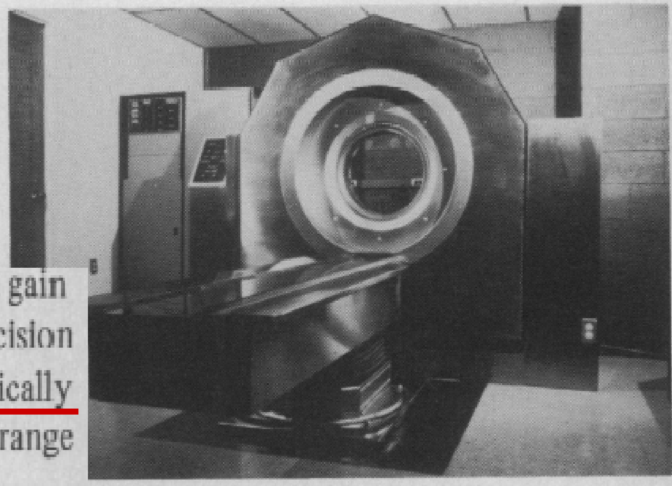

Fig. 1. Photograph of Super PETT I.

....

is not entirely settled, there seems to be agreement that a gain of several fold (2.5-4) can be obtained with TOF precision measurements of about 400-500 ps, which is practically achievable with modern technology, for objects in size range of 30-35 cm, in their transversal dimensions.

CONCLUSIONS AND DISCUSSION

The following, albeit preliminary, conclusions can be drawn. As predicted, the incorporation of photon time-of-flight information into the PET reconstruction process does substantially increase the signal-to-noise ratio in the reconstructed image for a timing resolution of about 500 ps. The measured

TOF today

1464 IEEE TRANSACTIONS ON NUCLEAR SCIENCE, VOL. 54, NO. 5, OCTOBER 2007

A Further Study of Timing With LSO on XP20D0 for TOF PET

T. Szczęśniak, *Member, IEEE*, M. Moszyński, *Fellow, IEEE*, A. Nassalski, *Member, IEEE*, P. Lavoute, and A. G. Dehaine

… a very good time resolution of 350 ± 12 ps with a single $4 \times 4 \times 20$ mm^3 LSO and the system realizing light readout by the two PMTs was reported.

New materials such as $LaBr_3$ could help the improvement of TOF PET instrumentation but the recent results seems to indicate a time resolution of about 500 ps* when measured in coincidence mode and Anger logic position readout.

* From: **Design of a lanthanium bromide detector for TOF PET**. Kuhn, A.; Surti, S.; Karp, J.S.; Raby, P.S.; Shah, K.S.; Perkins, A.E.; Muehllehner, G.; IEEE – NSS Conference Record, 2003 IEEE Vol. 3 (2003) 1953 – 1957

Silicon PhotoMultiplier = SiPM
The Ultimate dream??

SOLID STATE PHOTODETECTOR➔ SiPM: **Multicell Avalanche Photodiode** working in limited Geiger mode

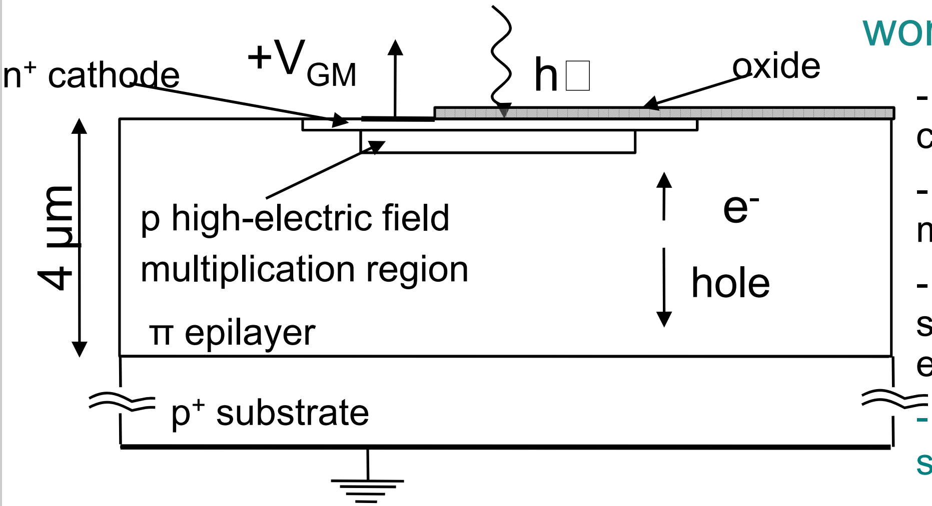

- 2D array of microcells: structures in a common bulk.
- Vbias > Vbreakdown: high field in mult. region
- Microcells work in Geiger mode: the signal is independent of the particle energy
- The SiPM output is the sum of the signals produced in all microcells fired.

-The photon is absorbed and generates an electron/hole pair

-The electron/hole diffuses or drifts to the high-electric field multiplication region

-The drifted charge undergoes impact ionization and causes an avalanche breakdown.

-Resistor in series to quench the avalanche (limited Geiger mode).

As produced at FBK-irst,Trento, Italy➔

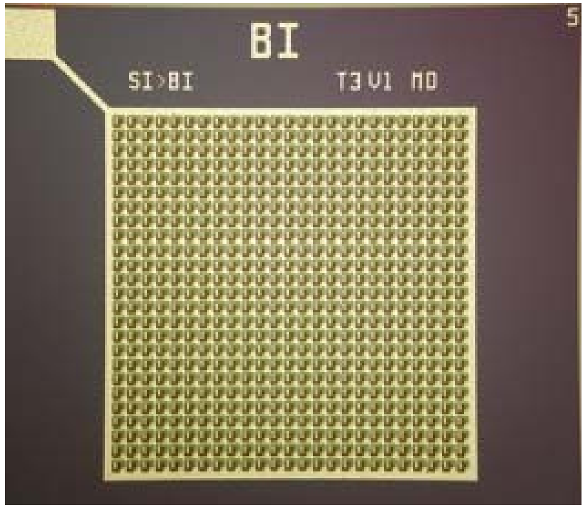

→High gain →Low noise → Good proportionality if $N_{photons} << N_{cells}$

Results: characterization

- PET History
- PET Physics and technology
- PSDs in PET: PMT
- PSDs in PET: solid state
- Advanced PET detectors: DOI and TOF
- **SiPMs for PET**
- Conclusions

FBK- irst (Trento, Italy) is developing SiPMs since 2005:

First detectors - Single SiPMs (2006)

First matrices 2x2 (2007)

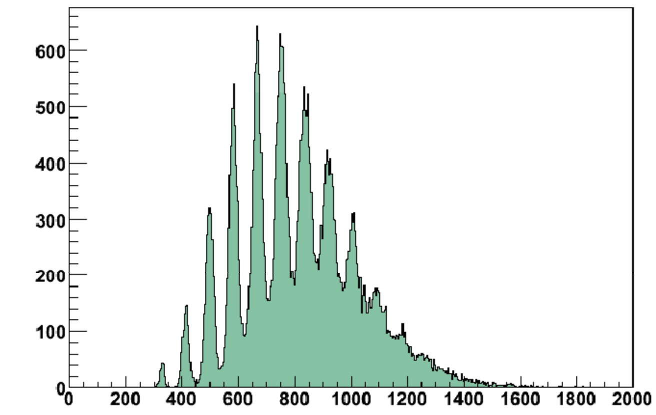

Breakdown voltage V_B ~ 30V, **very good uniformity.**

Single photoelectron **spectrum: well resolved peaks.**

Gain: ~10^6

- Linear for a few volts over V_{BD}.
- Related to the recharge of the diode capacitance C_D from V_{BD} to V_{BIAS} during the avalanche quenching. $G=(V_{BIAS}-V_B) \times C_D/q$

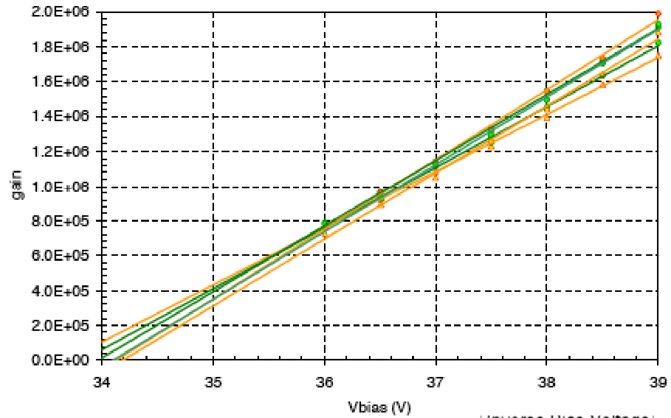

Dark rate:

- 1-3 MHz at 1-2 photoelectron (p.e.) level, ~kHz at 3-4 p.e (room temperature).
- Not a concern for PET applications.

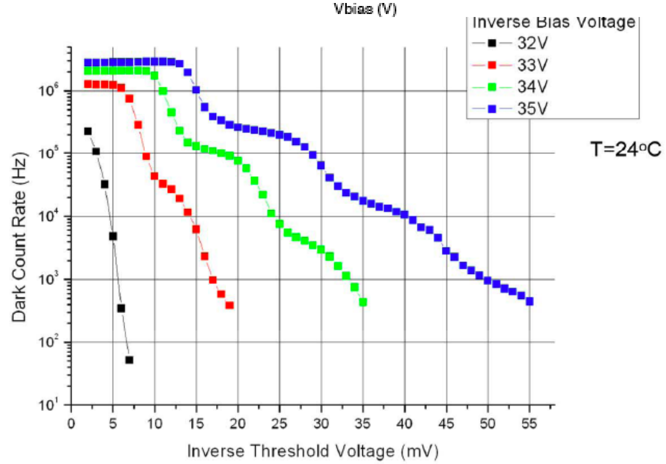

Results: intrinsic timing

Intrinsic timing measured at s.p.e level:
60 ps (σ) for blue light at 4V overvoltage.

SiPM illuminated with a pulsed laser with 60 fs pulse width and 12.34 ns period, with less than 100 fs jitter.

Two wavelengths measured:

λ = 400 ±7 nm and λ = 800 ±15 nm.

Time difference between contiguous pulses is determined.

The timing decreases with the number of photoelectrons as

1/√(Npe)➔ 20 ps at 15 photoelectrons.

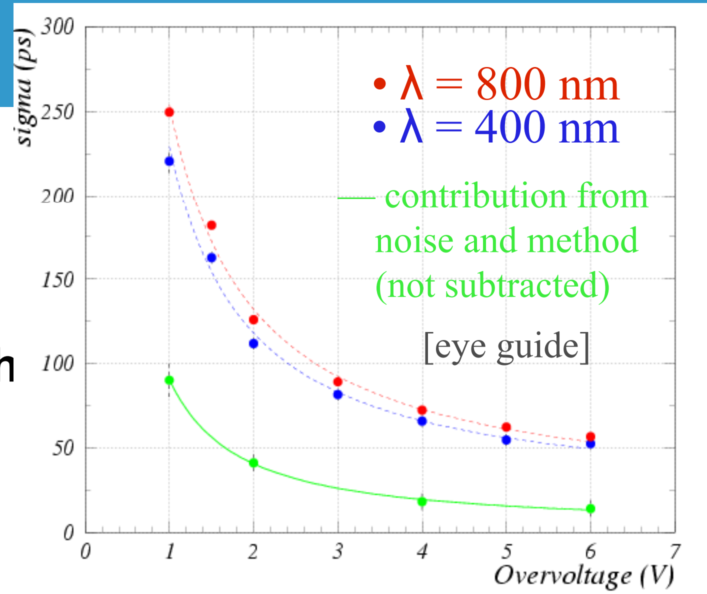

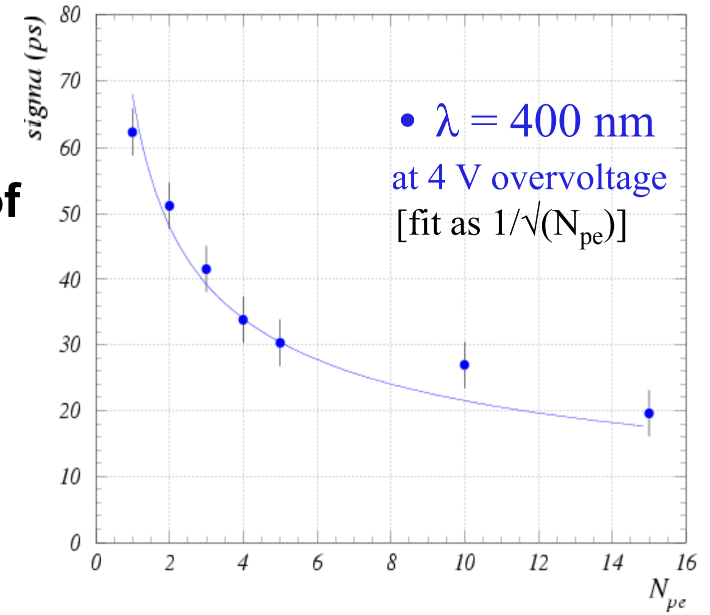

[G. Collazuol et al., VCI 2007, published in NIM A.]

Results: coincidence timing (TOF)

- PET History
- PET Physics and technology
- PSDs in PET: PMT
- PSDs in PET: solid state
- Advanced PET detectors: DOI and TOF
- SiPMs for PET
- Conclusions

Coincidence measurement with two LSO crystals (1x1x10 mm³) coupled to two SiPMs {Theory: Post and Schiff. Phys. Rev. 80 (1950)1113.}

$$\sigma \sim \frac{\sqrt{Q}\,\tau}{<N>}$$

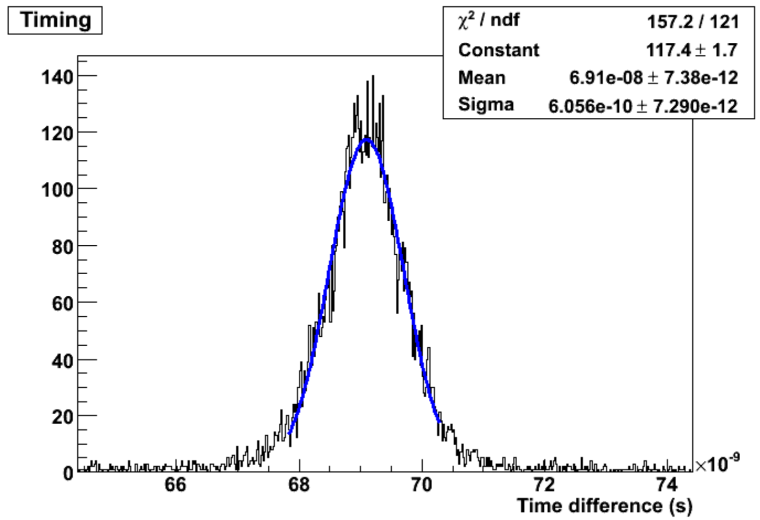

Where:

<N> = average number of photons: ~ 100 photons at the photopeak

Q = Trigger level: ~1 photoelectron.

τ = Decay time of the scintillator

For two scintillators in coincidence expected : => √2σ~ 630 ps .

Measured => ~ 600 ps sigma.

Measurements in agreement with what we expect!!

[G.Llosa,et al., Conf records of the IEEE NSS-MIC 2007, Honolulu,USA]

Results: energy resolution (ΔE/E)

- PET History
- PET Physics and technology
- PSDs in PET: PMT
- PSDs in PET: solid state
- Advanced PET detectors: DOI and TOF
- SiPMs for PET
- Conclusions

Setup:

- 2 LSO [1mm x 1mm x 10mm] crystals coupled to 2 SiPMs
- Home made amplifier board.
- Time coincidence of signals.
- VME QDC for DAQ.
- ^{22}Na source.

Energy resolution in coincidence: 20% FWHM.
(best result: 17.5 %)

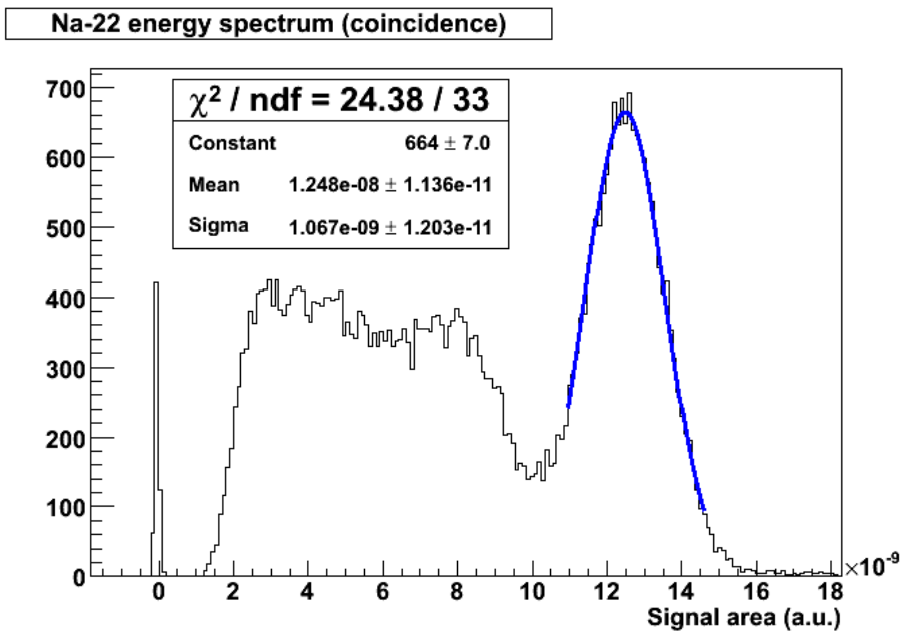

[G.Llosa et al, Conference Records IEEE NSS-MIC 2006, M06-88]

Results: New detectors (May 2007)

- PET History
- PET Physics and technology
- PSDs in PET: PMT
- PSDs in PET: solid state
- Advanced PET detectors: DOI and TOF
- **SiPMs for PET**
- Conclusions

Different geometry,size,microcell size and GF.

40x40μm^2 => GF 44%
50x50μm^2 => GF 50%
100x100μm^2 => GF 76%

circular

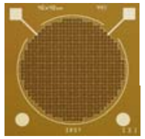

1mm ϕ

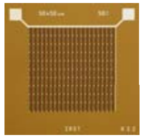

1x1mm^2

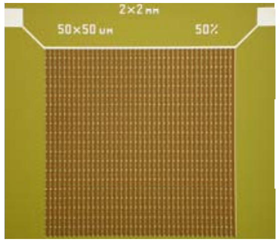

2x2mm^2

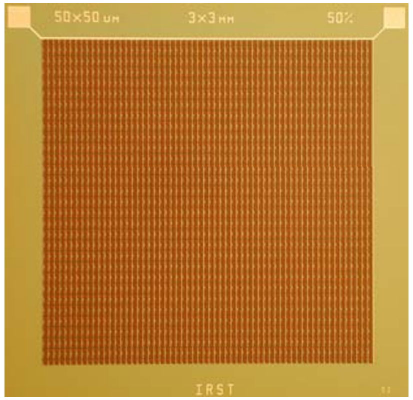

3x3mm^2 (3600 cells)

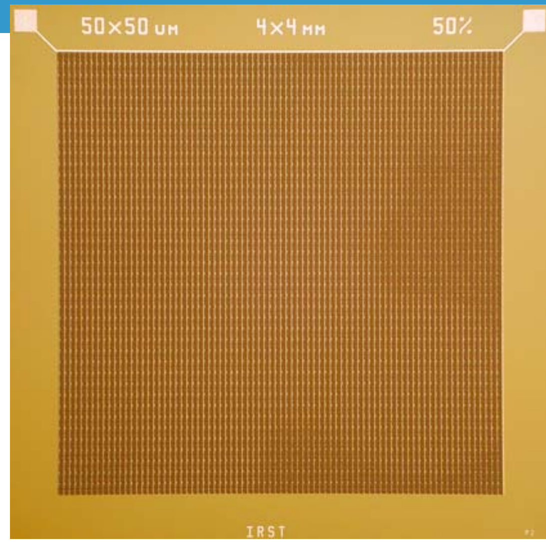

4x4mm^2 (6400 cells)

Matrices 16 elements (4x4)

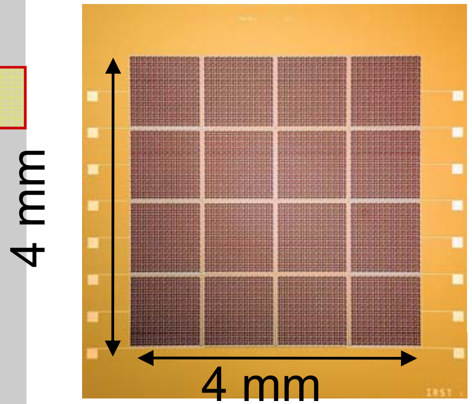

IV CURVES OF 9 MATRICES.

VERY UNIFORM BREAKDOWN POINT

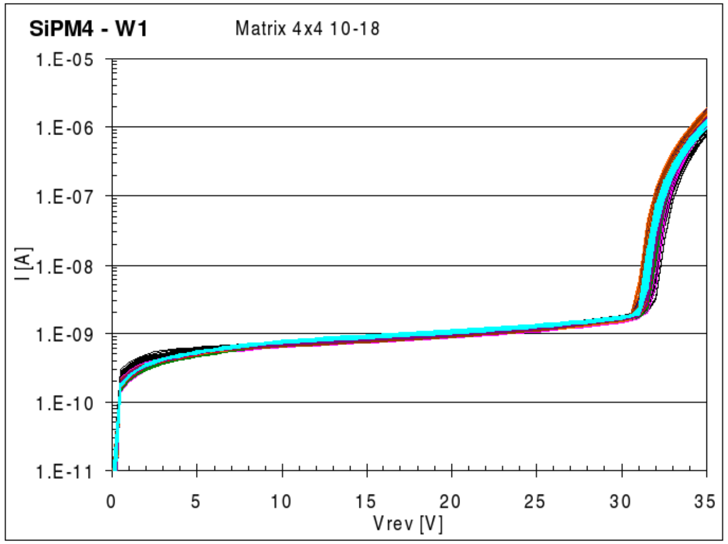

[C.Piemonte et al, Nuovo Cimento C, 2007 to be published]

Position determination

Hitmap for different source position with crystal array

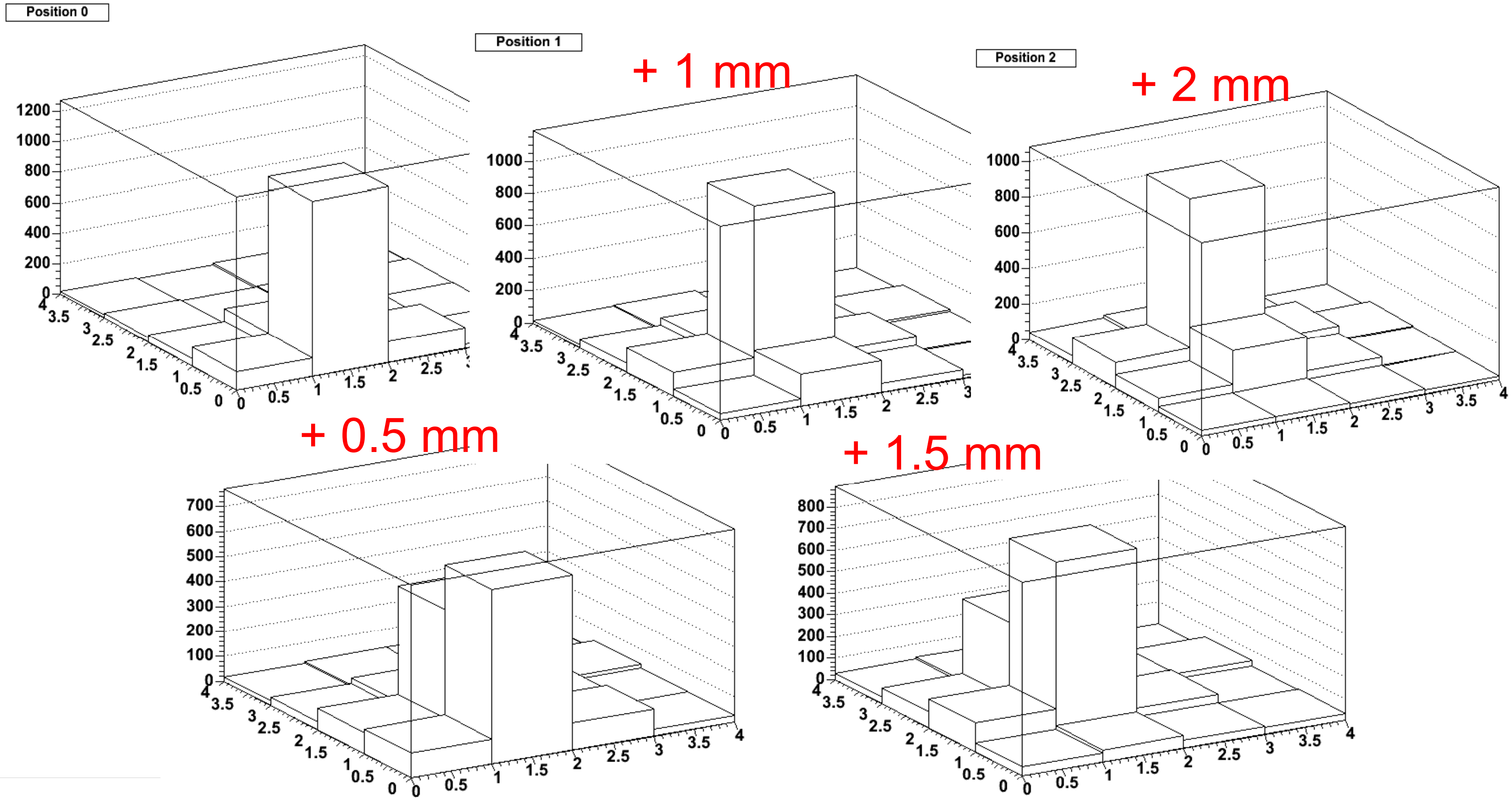

Results with continuous crystals

- PET History
- PET Physics and technology
- PSDs in PET: PMT
- PSDs in PET: solid state
- Advanced PET detectors: DOI and TOF
- **SiPMs for PET**
- Conclusions

Crystal 4 mm x 4 mm x 5 mm covering the whole 4x4 matrix.

Na-22 spectrum summing signals from all channels.

$\Delta V = 4V$

$\Delta E/E = 16\%$

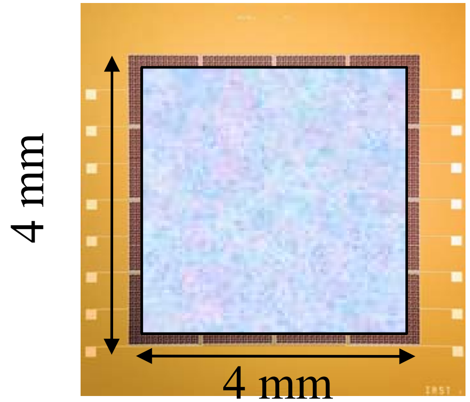

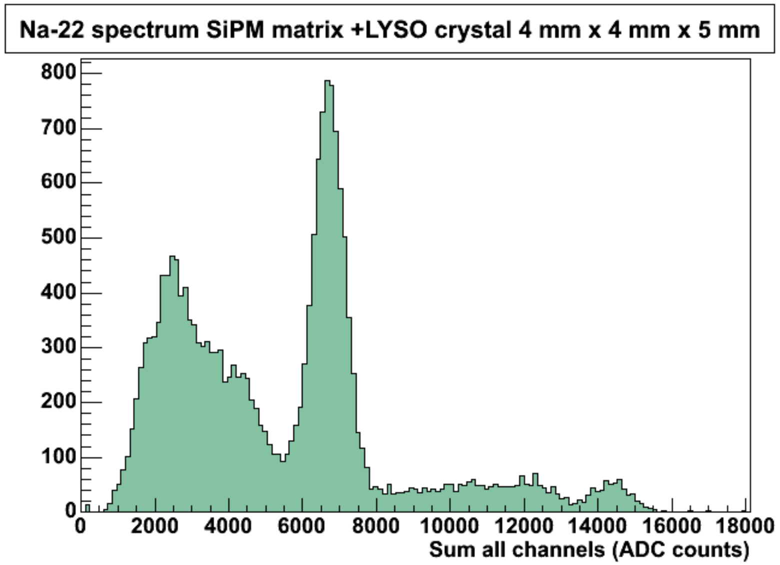

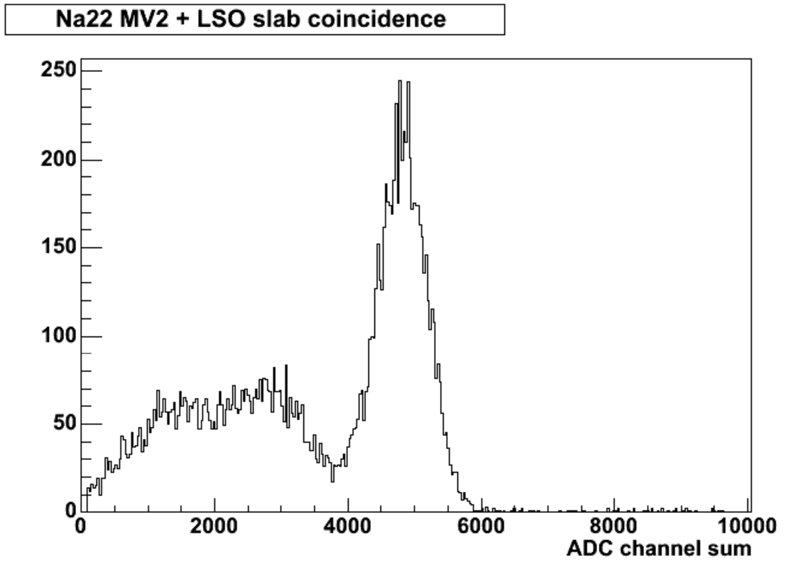

PET/MRI with APDs

- PET History
- PET Physics and technology
- PSDs in PET: PMT
- PSDs in PET: solid state
- Advanced PET detectors: DOI and TOF
- SiPMs for PET
- Conclusions

^{18}F-fluorodeoxyglucose - Human

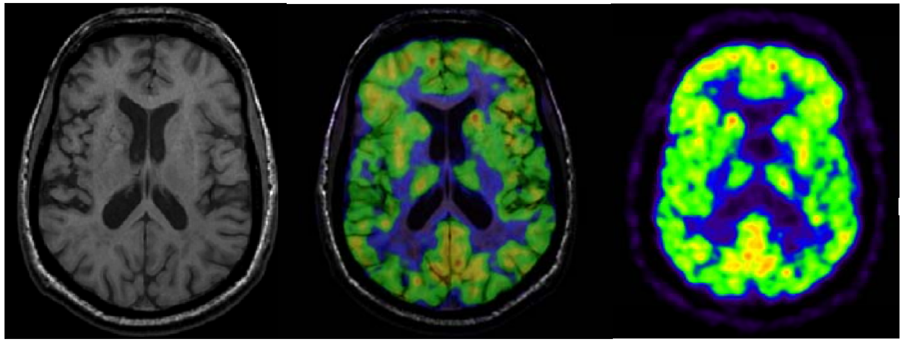

SIEMENS

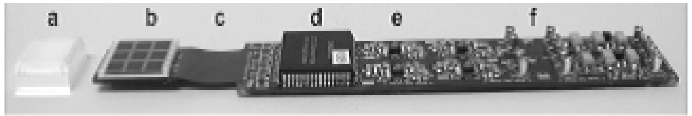

19 x 19 mm crystal block (a): 12 x 12 individual 1.5 x 1.5 x 4.5 mm crystals coupled via a 3 mm thick light guide to a monolithic 3 x 3 APD array (b) (Hamamatsu, Japan)

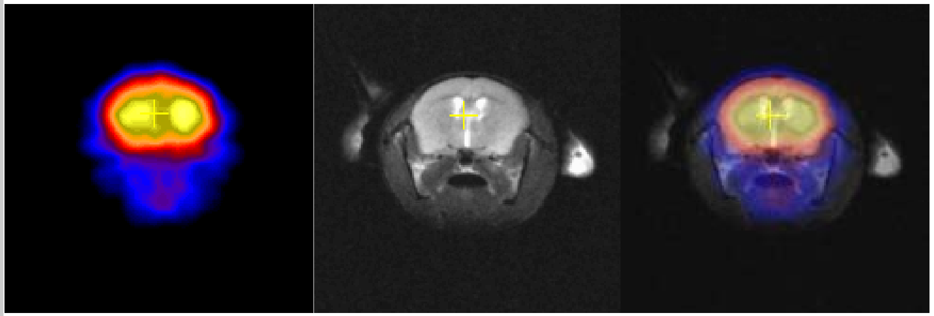

^{11}C-methylphenidate - Mouse

^{18}F-fluorodeoxyglucose - Mouse

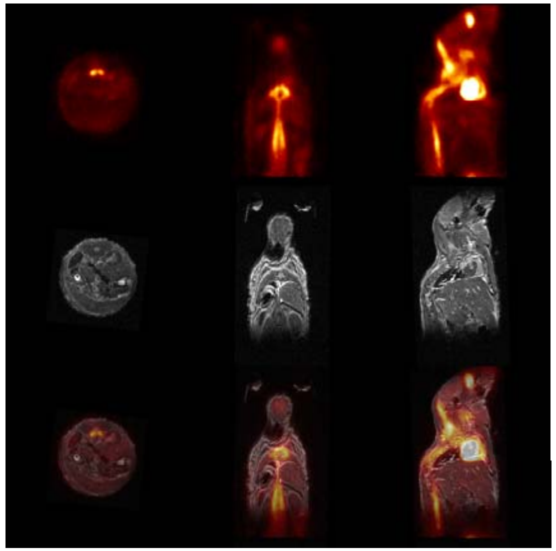

Courtesy Bernd Pichler

Results: tests of SIPM in MR system (MRI)

in collaboration with the Wolfson Brain Imaging Center, Cambridge, UK

S.p.e and ^{22}Na energy spectra acquired with gradients off (black line) and on (red line).

No real difference is appreciated in the data.

Differences in photopeak position is due to temp changes in the magnet

(apparent change in gain due to changes in breakdown voltage).

Pickup in baseline when switching on/off

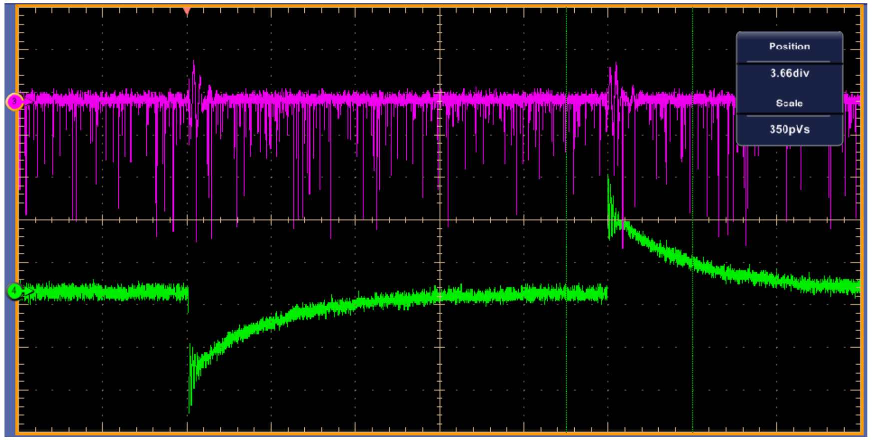

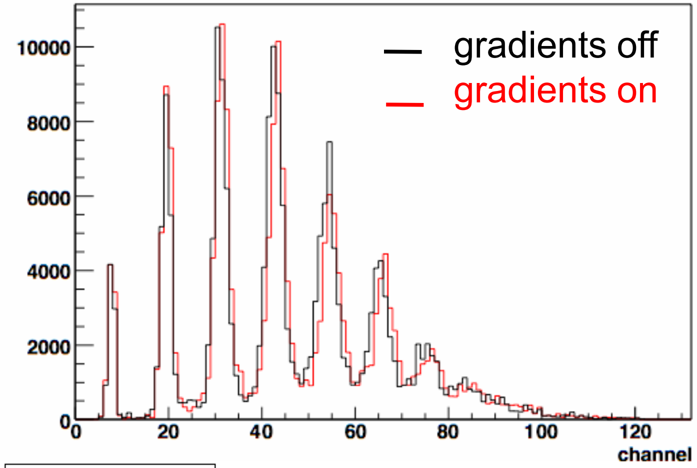

22^Na spectrum

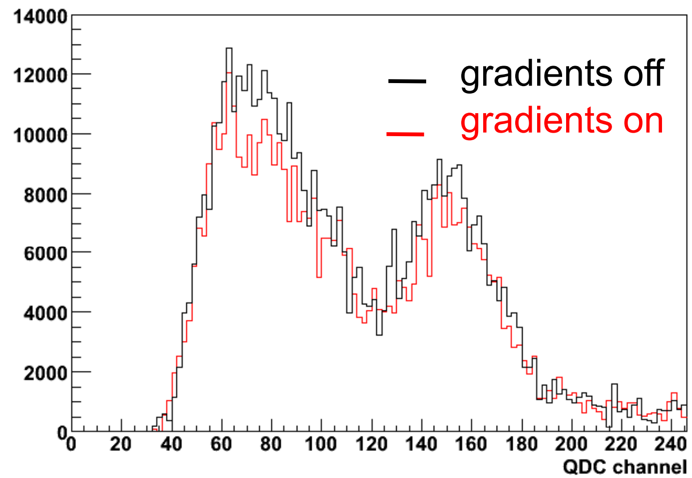

[R.C.Hawkes,et al. to be presented at IEEE, NSS-MIC 2007, Honolulu,USA]

Conclusion #1: photodetectors for clinical PET instrumentation

Clinical PET instrumentation seems to be scintillator oriented also for the future

After more than 20 years the block detector is going to be overcome by other approaches

The development of the electronic now is mature enough to open once again the possibility for a new rise of one-to-one coupling

TOF is growing slowly: faster scintillators and high quantum efficiency PhotoDetectors are required.

A multimodality approach (PET/MR) will be more and more requested in the clinical practice.

The SiPM seems to be the choice for future systems being MR compatible, compact and with high performance.

Conclusion #2: photodetectors for small animal PET instrumentation

Small animal PET instrumentation differs from clinical scanners for the use of higher intrinsic resolution photodetectors, mainly PSPMTs.

The one-to-one coupling and DOI measurement are already employed in some small animal scanners

Solid state detectors could be a valid alternative to the scintillator approach.

The multimodality is much required for small animal imaging.

The SiPM has all of the characteristics: speed, QE, granularity, flexibility, robustness for a successful implementation in small animal instrumentation.

Conclusion #3

SiPMs and SiPM matrices:

- Are well understood (available, reproducible, robust,...)
- Perform to SPECs (Fast, High PDE, MRI compatible,...)
- Geometry and performance can be tailored to the application!
- Are well suited for PET and also for SPECT applications (both pixellated and slab of scintillator)

BUT….. There is no free lunch!! They NEED:

- Dedicated ASIC (under development)
- Temperature control (sensor and feedback on the ASIC)
- Distributed readout (easily 10-50k channel)
- Low cost in the future [commercial cost now: ~100$ per mm^2]

Conclusions #4

- PET History
- PET Physics and technology
- PSDs in PET: PMT
- PSDs in PET: solid state
- Advanced PET detectors: DOI and TOF
- SiPMs for PET
- Conclusions

Quoted From: **"Recent developments in PET detector technology"**
Tom K Lewellen, Phys. Med. Biol. 53 (2008) R287–R317

"........Further, my crystal ball predicts that the winner for the ultimate PET detector design is likely to be a mosaic detector made up of elements consisting of slabs of crystal (perhaps 50 x 50 mm^2) viewed by arrays of SiPMs and supported by statistical-based estimation algorithms that locate events in the crystal slabs in three dimensions....."

→The design as in ref: **"A detector head design for small-animal PET with silicon photomultipliers (SiPM)",S. Moehrs, A.Del Guerra, et al. *Phys. Med. Biol.* 51(2006) 1113–27**

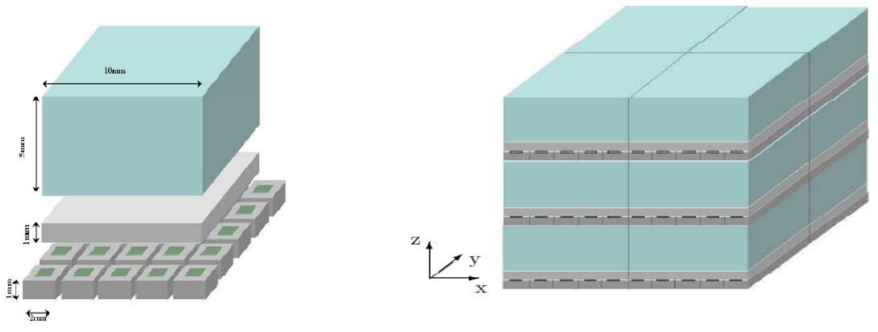

Acknowledgements

Functional Imaging and Instrumentation Group

Department of Physics"E.Fermi"

University of Pisa, Pisa, Italy

Francesca Attanasi (PhD student)
Antonietta Bartoli (Post-Doc)
Nicola Belcari (Research Assistant)
Gina Belmonte (PhD student)
Daniel Bonifacio (visiting PhD student)
Valter Bencivelli (Associate Prof)
Laura Biagi (Post-doc)
Maria G. Bisogni (Research Assistant)
Manuela Camarda (PhD Student)
Sebnem Erturk (PhD Student)
Serena Fabbri (PhD Student)
Alberto Del Guerra (Full Professor)
Gabriela Llosá (Marie Curie Fellow)
Sara Marcatili (PhD Student)
Sara Mattafirri (visiting PhD student)
Sascha Moehrs (Post-Doc)
Daniele Panetta (Post-Doc)
Michela Tosetti (Researcher)
Valeria Rosso (Associate Professor)
Sara Vecchio (PhD Student)

Thank you!